2

BNL-27699

CONF-800375--1

MASTER

KAON-NUCLEUS INTERACTIONS*

by

Carl B. Dover
Physics Department
Brookhaven National Laboratory**
Upton, New York 11973

* Invited paper presented at the Workshop on Low and Intermediate Energy Kaon Nucleon Physics, Istituto di Fisica, Rome, Italy, March 24-28, 1980.

** Supported by the U. S. Department of Energy under Contract No. DE-AC02-76CH00016.

KAON-NUCLEUS INTERACTIONS*

Carl B. Dover
Physics Department
Brookhaven National Laboratory**
Upton, New York 11973

* Invited paper presented at the Workshop on Low and Intermediate Energy Kaon Nucleon Physics, Istituto di Fisica, Rome, March 24-28, 1980.

** Supported by the U. S. Department of Energy under Contract No. DE-AC02-76CH00016.

Most of the emphasis at this meeting has been on the elementary interactions of kaons ($K^{\pm}$, K_L^{o}) with nucleons. I would like to shift the emphasis for a moment to a discussion of possibilities for the study of nuclear and hypernuclear structure physics with kaon beams[1-4]. With the availability of K^+ and K^- beams[3,4] at CERN, Brookhaven, and KEK in Japan, there has been increased interest in the last few years in kaon-nucleus physics, particularly in hypernucleus formation. I propose to review briefly the recent progress in hypernuclear physics, in particular the studies of Λ and Σ states via the strangeness-exchange (K^-,π^-) reaction. Prospects for future investigations with (proposed) intense kaon beams are also evaluated, for instance the production of high spin hypernuclei via the (π^+,K^+) reaction, and the formation of strangeness S = -2 hypernuclei ($\Lambda\Lambda$ or Ξ^-) by means of the (K^-,K^+) process. We close with a very brief resumé of elastic, inelastic and charge exchange reactions induced by the interaction of K^+ mesons with nuclei[5].

To appreciate the striking difference between K^- and K^+ interactions with nuclei, it is worthwhile to review the main features of the elementary $K^{\pm}N$ interactions.

The average interactions of K^+ and K^- with nucleons are very different in character. The low energy K^-N cross sections[6] for isospin I = 0, 1 are shown in Fig. 1. The average K^- cross section is roughly 40mb, typical of hadronic processes. The existence of a number of S = -1 Y^* resonances is evident from the data. In Fig. 2, we show for comparison the K^+N cross sections[7] for I = 0,1. In contrast to K^-N, the K^+N cross sections are small ($\simeq$ 10mb) and almost energy independent for

$p_{lab} \leq 700$ MeV/c, below the onset of inelastic processes.

The opposite strangeness $S = \pm 1$ for $K^{\pm}$ plays the dominant role in understanding the large cross section differences evident from Figs. 1 and 2. In Fig. 3, we illustrate[8] how $S = -1$ Y^* resonances are formed in a natural way in the quark model through the annihilation of a $q\bar{q}$ pair. The Y^* resonances correspond to ordinary low-lying three quark states. In contrast, we see from Fig. 3 that there is no corresponding quark annihilation process for K^+N, so possible intermediate states (exotic Z^* resonances with $S = +1$) cannot be composed of three quarks, the minimum complexity being $\bar{s}qqqq$.

Due to the qualitative differences in their elementary interactions with nucleons, the K^+ and K^- are quite distinct probes of the nucleus. One way of expressing this difference is in terms of the mean free path $\lambda = (\rho\sigma)^{-1}$ in nuclear matter. Here $\rho = 0.16\text{fm}^{-3}$ is the nuclear matter density and σ is the average total cross section $(\sigma_{K^{\pm}p} + \sigma_{K^{\pm}n})/2$. For K^-, we have $1\text{fm} \leq \lambda_{K^-} \leq 2\text{fm}$ for $p_{lab} \leq 800$ MeV/c, while for K^+ we obtain $5\text{fm} \leq \lambda_{K^+} \leq 7\text{fm}$. The K^+ mean free path is predicted to be very long[5], comparable to the size of a large nucleus like ^{208}Pb. The K^-, on the other hand, is a strongly absorbed particle in nuclei; its interactions are thus restricted to the nuclear surface.

The K^-, unlike the K^+, can transfer one or two units of strangeness to the nucleus. Some of the strangeness exchange reactions which lead to Λ and Σ hypernuclear formation are the following:

$$K^- + n \rightarrow \pi^- + \Lambda \text{ or } \pi^- + \Sigma^\circ$$
$$K^- + p \rightarrow \pi^+ + \Sigma^- \qquad (1)$$

Another reaction which could be used to produce hypernuclei, although under quite different kinematical conditions, is associated production

$$\pi^+ + n \rightarrow K^+ + \Lambda \qquad (2)$$

Finally, Ξ^- hypernuclei (S = -2) can be produced via the reaction

$$K^- + p \rightarrow K^+ + \Xi^- \qquad (3)$$

Systems containing a Σ or Ξ particle are unstable with respect to strong conversion processes of the type

$$\Sigma^- + p \rightarrow \Lambda + n$$
$$\Xi^- + p \rightarrow \Lambda + \Lambda \qquad (4)$$

One of our tasks will be to estimate the widths of Σ and Ξ states arising from such reactions.

Reactions (1) and (2) are distinguished by the momentum transfer q, for a nuclear target at rest in the lab system. The value of q at $\theta_{LAB} = 0°$ is plotted in Fig. 4 as a function of meson incident lab momentum. For the reaction (K,π), there exists a "magic momentum" such that the Λ or Σ is created at rest in the lab. The importance of this fact for hypernuclear production was emphasized by Feshbach and Kerman[9]. The Λ or Σ at rest has a sizable "sticking probability" for remaining bound to the nucleus. The excitation of 0^+ configurations where the Λ or Σ coherently replaces the last valence nucleon (i.e., occupies the same shell model orbit as vacated by the nucleon) is favored. The magic momenta are about 300 MeV/c for Σ° and 530 MeV/c for Λ production. Currently, kaon beams in this momentum region are not available, so experiments are done in the 700-900 MeV/c region. However, from Fig. 4, we see that q remains small ($\leq$ 50 MeV/c) compared to the nucleon Fermi momentum p_F = 270 MeV/c for $p_{K^-} \leq$ 800 MeV/c, so coherent substitutional processes are important at 0° in the whole low momentum region. The situation is quite different for the $\pi^+ n \to K^+ \Lambda$ reaction, as seen in Fig. 4. Here $q \geq p_F$ for all momenta of interest. The <u>low spin</u> states emphasized by the (K^-,π^-) process will be only very weakly excited in (π^+,K^+). Instead, the Λ has a measurable "sticking probability" only in <u>high spin</u> configurations in (π^+,K^+), because its large linear momentum can only be matched to a correspondingly high angular momentum. The same is true for a Ξ^- produced in a (K^-,K^+) reaction. We return later to a discussion of these reactions.

The (K^-,π^-) experiments[10-12] which have been done to date with nuclear targets have had energy resolution in the range $\Delta E \simeq 2.5$ -6 MeV. With such coarse resolution experiments, one sees only the energy-averaged gross structure of hypernuclei; that is, Λ particle-neutron hole (Λn^{-1}) states. As an example, consider the hypernucleus ${}^{16}_{\Lambda}O$. The ground state doublet of ${}^{16}_{\Lambda}O$ arises by replacing the neutron in the last valence orbit $(nP_{1/2})$ by a Λ in the lowest lying orbit $(\Lambda S_{1/2})$. We thus obtain

$$(\Lambda S_{1/2} \otimes nP^{-1}_{1/2})\ 0^-,1^- \tag{5}$$

In hypernuclei, the natural parity member of the ground state doublet ($\pi = (-)^J$) lies lowest in energy. The very small splitting of the doublet cannot be resolved experimentally. Note that the cross section to the 0^- state is essentially zero in the (K^-,π^-) reaction, except for parity violating effects. In general, (K,π) cross sections to other unnatural parity states ($1^+,2^-,3^+$, etc.), which rely on spin-flip amplitudes for their production, are also calculated[13] to be small, even for $\theta_L \neq 0°$. We neglect these in the following. The low-lying excited natural parity states in ${}^{16}_{\Lambda}O$ are

$$(\Lambda S_{1/2} \otimes n\ P_{3/2}^{-1})_{1^-}$$

$$(\Lambda P_{1/2,3/2} \otimes n\ P_{1/2}^{-1})_{0^+,2^+} \qquad (6)$$

$$(\Lambda P_{1/2,3/2} \otimes n\ P_{3/2}^{-1})_{0^+,2^+,2^+}$$

The experimental spectrum for the (K^-,π^-) reaction on ^{16}O and ^{40}Ca targets[10,11] is shown in Fig. 5. The CERN 0° data for ^{12}C, ^{32}S and ^{209}Bi are given in Fig. 6. In very light hypernuclei, such as ${}^{12}_{\Lambda}C$ and ${}^{16}_{\Lambda}O$, the narrow peaks due to particular Λ particle-neutron hole states (Λn^{-1}) dominate the spectrum. For heavier systems, the quasielastic part of the spectrum becomes relatively more important. This process involves the emission of a Λ into the continuum. This leads to a sizable "background" cross section, for instance in ${}^{209}_{\Lambda}Bi$, which makes it difficult to resolve individual hypernuclear states.

In the distorted wave impulse approximation (DWIA), the (K^-,π^-)

cross section at $\theta_L = 0°$ on a spin zero target takes the form

$$\frac{d\sigma}{d\Omega}(J^\pi) = \left(\frac{d\sigma}{d\Omega}\right)^{0°}_{K^- n\to\pi^-\Lambda} N^J_{eff} \tag{7}$$

where the final Λn^{-1} state has quantum numbers $|J^\pi\rangle = (\Lambda\ell_p j_p \otimes n(\ell_h j_h)^{-1})_{J^\pi}$. In Eq. (7), $(d\sigma/d\Omega)^{0°}_{K^- n\to\pi^-\Lambda}$ is the 0° lab cross section for the elementary $K^- n\to\pi^-\Lambda$ process, and N^J_{eff} is the effective number of neutrons, given by[14]

$$N^J_{eff} = (2J+1)\ (2j_p+1)\ (2j_h+1) \begin{pmatrix} j_p & j_h & J \\ \frac{1}{2} & -\frac{1}{2} & 0 \end{pmatrix}^2 F_J(q) \tag{8}$$

Note that at 0°, only natural parity states are excited, so that $\ell_p+\ell_h+J$ must be even. The form factor $F_J(q)$ involves the radial overlap of the Λ and n^{-1} wave functions with kaon and pion distorted waves:

$$F_J(q) = \left(\int_0^\infty r^2 dr\ R_p(r)\ R_h(r)\ \hat{j}_J\ (r)\right)^2 \tag{9}$$

In plane wave approximation (PWA), $\hat{j}_J$ reduces to the usual spherical Bessel function $j_J(qr)$. The formulae (7)-(9) can easily be generalized[5] to $\theta_L \neq 0°$.

Near the "magic momentum" for the (K^-,π^-) reaction, $\theta_L = 0°$ corresponds to $q \simeq 0$. In PWA, we see immediately from Eq. (9) that only $F_o(q)$ differs from zero for $q \simeq 0$; thus 0^+ states will dominate for $\theta_L = 0°$. As we increase θ_L, q also becomes larger and $F_o(q)$ decreases; other form factors $F_J(q)$ for $J\neq 0$ come into play. The higher spin states not seen at 0° can be revealed by their characteristic angular distributions.

The goal of the theory is to predict the values of N_{eff}^{J} for various Λn^{-1} configurations, i.e. the (K^-,π^-) "strength function". Some typical results due to Bouyssy[15] are shown in Fig. 7. The contributions of individual Λn^{-1} states are indicated by dashed lines; they have been spread out in energy to simulate the results of a coarse resolution experiment. The envelope corresponding to the sum of all Λn^{-1} contributions is shown as a solid line, with the corresponding CERN data displayed in the inset. The low spin states are seen to dominate, and the comparison with data enables one to assign experimental peaks to particular Λn^{-1} states, at least in light hypernuclei, where the Λn^{-1} configurations of a given spin J are well spaced and only weakly admixed[14,15] by the residual ΛN interaction. The positions of the Λn^{-1} peaks are close to the unperturbed particle-hole energies. The n^{-1} single particle energies are taken from observed separation energies, and information on the Λ binding in the $S_{1/2}$ state is available from emulsion data on hypernuclear ground states. To predict the Λ binding energies in excited states, we need a model for the single particle potential $V_\Lambda(r)$ in a hypernucleus. We take a conventional Woods-Saxon form

$$V_\Lambda(r) \;=\; -V_o^{\Lambda} f(r) + V_{LS}^{\Lambda}\, \underset{\sim}{\ell} \cdot \underset{\sim}{\sigma}_\Lambda \left(\frac{\hbar}{m_\pi c}\right)^2 \frac{1}{r}\,\frac{df(r)}{dr} \qquad (10)$$

with $f(r) = (1 + \exp\,(r-R)/a)^{-1}$. The geometrical parameters $R = r_o A^{1/3}$, $r_o = 1.1$fm, $a = 0.6$fm are assumed to be similar to those for the nucleon potential. The depth parameters V_o^{Λ} and V_{LS}^{Λ} for the central and spin-orbit potentials have been determined[17] by a fit to the observed peak positions in the (K^-,π^-) reactions. The results are[17]

$$V_o^\Lambda \simeq 32 \pm 2 \text{ MeV}$$
$$V_{LS}^\Lambda \simeq 4 \pm 2 \text{ MeV} \quad (11)$$

The depth V_o^Λ is consistent with the emulsion results[16]. The new information gained from the CERN (K,π) data is the value of V_{LS}^Λ, which is much smaller than the value $V_{LS}^N \simeq 20$ MeV for nucleons. The fact that the Λ spin-orbit potential is small can be seen, for instance, from the $^{16}_\Lambda O$ spectrum of Fig. 5. The observed splitting between the $({}_\Lambda p_{3/2} \otimes n\, p_{3/2}^{-1})_{0^+}$ and $({}_\Lambda p_{1/2} \otimes n\, p_{1/2}^{-1})_{0^+}$ configurations, about 6MeV, can be attributed to the nucleon spin-orbit splitting, with no need for a large value of V_{LS}^Λ. Similar conclusions follow from an inspection of the $^{40}_\Lambda Ca$ spectrum in Fig. 5.

The Λ spin-orbit potential has been the object of some recent theoretical work[18,19,20], based on meson exchange models or the quark-gluon picture. The general conclusion of these authors is that V_{LS}^Λ should be small. Note, however, that the older analysis of p-shell hypernuclei due to Dalitz, Gal and Soper[21] yielded a large spin-orbit potential for the Λ, of opposite sign to that for a nucleon.

The CERN data at 0° are useful for determining the single particle potential of a Λ in a nucleus. These properties can already be determined from the low-spin part of the hypernuclear spectrum. The presence of higher spin states ($J \geq 2$) can only be established by measuring the (K^-,π^-) angular distributions. In a recent experiment[12] at the Brookhaven AGS, the angular distributions in Fig. 8 were obtained for the reaction $^{12}C(K^-,\pi^-)^{12}_\Lambda C^*$ at an incident momentum of 800 MeV/c. The data have been interpreted in Ref. (13) in DWIA. The angular shape for the ^{12}C ground state, with a peak at about 10°, is characteristic of a 1^- state. This is what one anticipates from the $({}_{\Lambda}S_{1/2} \otimes n\, P_{3/2}^{-1})_{1^-}$ configuration. The angular distribution for the group of states at 11 MeV excitation requires more interpretation. One expects the $({}_{\Lambda}P_{1/2} \otimes n\, P_{3/2}^{-1})2^+$ and $({}_{\Lambda}P_{3/2} \otimes n\, P_{3/2}^{-1})_{0^+,2^+}$ states to lie in this region of excitation. A coarse resolution experiment cannot separate these. If the Λ spin-orbit potential is indeed small, the energy splittings of the $0^+,2^+,2^+$ triplet come only from the residual ΛN interaction, which typically produces splittings of 1 MeV or less. Thus the data shown in the lower half of Fig. 8 reflect the summed strength for the $0^+,2^+,2^+$ states. The presence of the 2^+ excitations is revealed as a shoulder in the angular distribution in the region from 10° to 20°. The calculated contribution from the 0^+ state alone is several orders of magnitude below the data in this region. The DWIA theory[13] gives a good account of the shape of the angular distribution. This is sensitive to the relative size of the 0^+ and 2^+ contributions, which the theory gives correctly. Agreement in absolute size of the (K,π) cross sections requires multiplication of the theoretical values by an overall normalization factor of about 1/2. The origins of this discrepancy are discussed in Ref. (13). In any case, the data in Fig. 8 provide clear evidence for the presence of the expected 2^+ strength, not seen in the 0° data.

The CERN group has also investigated the $(K^-,\pi^{\pm})$ reactions in the Σ region[22]. Some of their results are shown in Fig. 9 for the $^9Be\ (K^-,\pi^-)^9_{\Lambda}Be$ reactions at 720 MeV/c. The incident momentum is chosen to correspond to a peak in the elementary $K^-n \to \pi^- \Sigma^\circ$ process. The presence of (unbound) Σ states is suggested by the structures located within 20 MeV of the threshold corresponding to zero Σ binding ($B_\Sigma = 0$). Since the momentum transfer q is still reasonably small ($\simeq$ 130 MeV/c), we expect that these states would correspond to 0^+ or 1^- excitations. The surprising feature is the narrow width observed for these states ($\Gamma_\Sigma \lesssim 10$ MeV). It had been assumed that the strong conversion mechanism $\Sigma N \to \Lambda N$ would lead to very broad Σ states ($\Gamma \gtrsim 30$ MeV). A rough estimate of the Σ width in nuclei can be obtained from the perturbation theory result

$$\Gamma_\Sigma \approx (v\sigma)^{AV}_{\Sigma\bar{p}\to\Lambda n} \int_0^\infty \rho_p(r)\, u^2_{n\ell}(r) dr \qquad (12)$$

where $u_{n\ell}(r)$ is the Σ radial wave function, $\rho_p(r)$ is the proton density and $(v\sigma)^{AV}$ is the Fermi-averaged $\Sigma^- p \to \Lambda n$ cross section, v being the relative velocity. The experimental data[23] on the $\Sigma^- p \to \Lambda n$ process may be parametrized in the form

$$(v\sigma)_{\Sigma^- p \to \Lambda n} \approx (v\sigma)_o/(1 + \alpha v) \qquad (13)$$

where $(v\sigma)_o \simeq 65$ mb, $\alpha \simeq 20$. For a Σ^- at rest in the nucleus, the Fermi averaging over the nucleon motion yields $(v\sigma)^{AV}_{\Sigma^- p\to\Lambda n} \simeq 14$ mb. Note that $(v\sigma)^{AV}$ is only about 1/5 of the threshold value $(v\sigma)_o$, which was used in early estimates of the Σ width. Using the smaller value $(v\sigma)^{AV}$, we get typical widths[24]

$$\Gamma_\Sigma^{1S} \simeq 23 \text{ MeV}, \ \Gamma_\Sigma^{1p} \simeq 13 \text{ MeV} \qquad (14)$$

for ${}^{12}_{\Sigma}C$. For the 1P Σ-state, the value of Γ_Σ in Eq. (14) is already tantalizingly close to the width of the structures seen in Fig. 9.

Additional reduction[25] of the Σ width can arise in light nuclei because the low-energy $\Sigma N \to \Lambda N$ conversion mechanism is strongly spin and isospin dependent (the $^3S_1$, $I = 1/2$ channel dominates). In systems like $^{12}_{\Sigma}C$ and $^{7}_{\Sigma}Li$, the "core" seen by the Σ is not spin-isospin saturated. Thus the matrix element of the $\Sigma N \to \Lambda N$ amplitude between Σ and Λ hypernuclear wave functions will differ from that obtained by neglecting the spin-isospin dependence (as done in Eq. (12)). One can thus obtain either larger or smaller widths than from Eq. (12). Detailed estimates of Σ widths have been carried out in Ref. (25). It was found that 0^+ states with $I = 3/2$ enjoy an appreciable suppression of the Σ width relative to the limit where spin-isospin effects are ignored. The width suppression effect is limited to only a few states: 1^- and 0^+, $I = 1/2$ states in $^{12}_{\Sigma}C$ and $^{16}_{\Sigma}O$ are broadened rather than narrowed. Definite predictions for the quantum numbers of narrow Σ states in light nuclei have been made[25]. These cannot be firmly established on the basis of the 0° data alone; angular distributions are required.

A particularly interesting case is that of $^{16}_{\Sigma}O$. The two states which are candidates for narrow structure[25] are the $I=3/2$, $({}_{\Sigma}P_{3/2} \otimes n\ P^{-1}_{3/2})_{0^+}$ and $({}_{\Sigma}P_{1/2} \otimes n\ P^{-1}_{1/2})_{0^+}$ configurations. If the spin-orbit potential for the Σ is weak, these two states are predicted to be fairly broad and separated by about 6 MeV. On the other hand, if the Σ spin-orbit potential is comparable to that of the nucleon, the two 0^+ states will strongly mix and <u>one</u> of the diagonalized configurations carries almost all of the (K,π) strength. We then expect <u>one</u> quite narrow 0^+, $I = 3/2$ state in $^{16}_{\Sigma}O$. No data on $^{16}_{\Sigma}O$ is yet available to test this prediction. For Σ

states, it is important to measure both the (K^-,π^-) and the (K^-,π^+) reactions; the latter process filters out the I = 1/2 states.

There have also been some recent measurements of hypernuclear γ rays, in particular for ${}^4_\Lambda H$, ${}^4_\Lambda He$ (26) and for ${}^8_\Lambda Li$ (27). The importance of γ ray measurements has been emphasized by Dalitz and Gal[28]. The case of ${}^4_\Lambda H$, ${}^4_\Lambda He$ is interesting, since it bears on the question of charge symmetry breaking. Earlier experiments were interpreted in terms of a sizable $\Sigma^\circ - \Lambda$ mixing, but the more recent results[26] require much less violation of charge symmetry. The results for ${}^8_\Lambda Li$ can be compared with earlier predictions[28]. The theoretical results are sensitive to the spin dependence of the ΛN residual interaction, which we hope to test with such data.

The previous sections have been devoted to a brief review of the experimental data on hypernuclei. One may now ask: what are the future prospects for kaon physics? Several projects for improved kaon beams are in the planning or development stage. At CERN, a K^- beam at 450 MeV/c is under construction[30]. The low momentum will be more favorable for the study of Σ hypernuclei, since one is then closer to the "magic momentum" (see Fig. 4). A workshop group is developing a proposal for a dedicated kaon beam at the Brookhaven AGS with an intensity of perhaps 50 times current values (2×10^4 kaons/burst). Such a proposal could also include an intense pion beam in the 1 - 1.5 GeV/c range. There are also longer range discussions under way, for instance at LAMPF and TRIUMF, concerning the possibility of a "kaon factory". Some of these considerations were reviewed at the recent Kaon Workshop[31] at Vancouver.

In view of this discussion, it is important to provide a physics justification for a new kaon facility. I will mention here only a few of the unique possibilites for kaon physics. A number of other topics have also been explored, for which the reader is referred to the literature[31-34].

In heavy hypernuclei, we expect that collective "strangeness analog resonances" (SAR) will be formed[35]. As for isobaric analog states, the SAR involve a coherent superposition of Λn^{-1} states coupled to $J^{\pi} = 0^{+}$. In a somewhat idealized model[35], the SAR wave function remains antisymmetric with respect to the interchange of the Λ with any neutron, even though the Λ does not need to satisfy the Pauli principle. Theoretical calculations[36] indicate a tendency to develop such collective states in heavy nuclei. Since the quasielastic contribution to the (K^{-},π^{-}) reaction is large in heavy nuclei (see ${}^{209}_{\Lambda}$Bi in Fig. 6), experiments with better energy resolution will be required to see these narrow collective structures. These experiments will become feasible if new intense kaon beams become a reality.

In addition to the SAR, other "supersymmetric" configurations should exist in hypernuclei[37]. These states are predicted to lie well below the analog states (by 10-20 MeV) and correspond to symmetries that cannot be realized in ordinary nuclei because of the Pauli principle. For example, consider the $(1p)^5$ configuration outside the closed (1S) shell. The orbital permutation symmetry for the ground state of ^{9}Be is dominantly [41], which then also holds for the SAR in ${}^{9}_{\Lambda}$Be*. However, "supersymmetric" states of ${}^{9}_{\Lambda}$Be* also exist with orbital symmetry [5]; these states permit more relative s-state bonds than [41] states, and hence they lie lower in energy than the SAR. The ${}^{9}_{\Lambda}Be^{*}$ excitations may be grouped[37] into SU(6) multiplets, if one neglects the spin dependence of ΛN and NN forces. The SU(6) symmetry would imply that a number of non-analog states would be roughly degenerate with the SAR, leading to an interesting fine structure arising from the distribution of the strength of the SAR over these states. Data with much better energy resolution are required to see this fine structure. The search for such approximate symmetries in hypernuclear spectra is an exciting prospect for kaon physics.

Previously, we have discussed the simple Λ particle-neutron hole model for hypernuclei. Experiments with poor energy resolution are sensitive only to this gross Λn^{-1} structure. The next generation of experiments should be able to detect "core excited" states in hypernuclei. For example, Dalitz and Gal[28] have estimated the (K,π) cross section to the "core excited" states in ${}^{12}_{\Lambda}C$. In particular, a 1^- state consisting of ${}_{\Lambda}S_{1/2}$ coupled to the low-lying $1/2^-$ state in ${}^{11}C$ was predicted to lie about 3-4 MeV above the ${}^{12}_{\Lambda}C$ ground state, and to be populated with appreciable intensity in the (K^-,π^-) reaction. No evidence for this state was seen in the BNL data[12]; possible explanations for its absence are discussed in Ref. (13). These "core excited" states may also be viewed as arising from ground state correlations in the target, i.e. ${}^{12}_{\Lambda}C$ is a poor "closed shell", containing appreciable two-particle-two-hole correlations. Particle-hole excitations may also be created by inelastic scattering of the kaon or pion. Such dynamical effects can influence cross section estimates based on pre-existing ground state correlations.

The (K,π) reaction has been exploited to produce low spin hypernuclear states. The cross reaction (π,K) has recently been discussed[38] as a possibility for producing hypernuclei. Since the momentum transfer for $\pi^+ n \to K^+ \Lambda$ is large, as per Fig. 4, associated production will preferentially populate <u>high spin</u> states, nicely complementing the (K,π) measurements. An attractive experimental feature of the (π,K) process is the availability of large pion fluxes, typically 10^4 π's per K at the Brookhaven AGS. This permits the measurement of much smaller cross sections (1 μb/st is accessible) than for (K,π) with current beam intensities.

The configurations which are predicted[38] to dominate the (π,K) reaction are the natural parity "stretch states" obtained by coupling Λn^{-1} to spin $J = \ell_p + \ell_h$. If we consider nodeless oscillator wave functions for which $R_{1\ell}(r) \sim (r/b)^{\ell} \exp(-r^2/2b^2)$, the form factor $F_J(q)$ of Eq. (9) becomes

$$F_J(q) = \frac{z^J e^{-z}}{[(J+1)!!]^2} \tag{15}$$

where $z = (bq)^2/2$. Note that $F_J(q)$ vanishes at $q = 0$ for $J \neq 0$ and assumes its peak value for

$$J = (bq)^2/2 \tag{16}$$

The condition (16) represents the <u>optimum matching</u> of momentum transfer q and total spin J for the oscillator model. Note that $\theta_L = 0°$ corresponds to a large value $q = q_o$; values of $q<q_o$ are not accessible to experiment. The value q_o usually exceeds the optimum value $(2J)^{1/2}/b$ of Eq. (16), so that one is already past the peak of $F_J(q)$ for $\theta_L = 0°$, and the (π^+,K^+) cross section is a decreasing function of θ_L.

The question now arises: What is the highest spin Λn^{-1} state that one can manufacture in a given hypernucleus? If one assumes the potential $V_\Lambda(r)$ of Eq. (10), the spectrum of Λ single particle states can be calculated[38]. One can also seek guidance from Hartree-Fock calculations[39] for Λ hypernuclei. For systems with A>40 or so, the Λ orbit corresponding to the last bound nucleon orbit is a single particle resonance in the continuum. For typical systems like ^{48}Ca, ^{90}Zr, ^{138}Ba and ^{208}Pb, which have closed $j = \ell + 1/2$ neutron shells with $\ell = 3,4,5$ and 6, respectively, the corresponding Λ orbits lie at roughly 5-6 MeV in the continuum. The elastic width of these Λ states becomes narrower as A increases ($\Gamma_{EL} \simeq 2.4$ MeV for the 1f in $^{48}_{\Lambda}$Ca, $\Gamma_{EL} \simeq 0.3$ MeV for the 1i in $^{208}_{\Lambda}$Pb), so they should be observable as relatively narrow Λn^{-1} states, even though they are unbound. The highest spin narrow Λn^{-1} states that we anticipate are then obtained by coupling these single particle resonances to n^{-1} states: $^{28}_{\Lambda}$Si, $^{48}_{\Lambda}$Ca, $^{90}_{\Lambda}$Zr, $^{138}_{\Lambda}$Ba, and $^{208}_{\Lambda}$Pb are good candiates, since n^{-1} also has high spin. We can also couple the Λ in the next lowest orbit to n^{-1}, giving states with one less unit of J. We find

$$\begin{aligned}
{}^{28}_{\Lambda}\mathrm{Si}:\ & ({}_{\Lambda}d_{3/2,5/2} \otimes {}_{n}d^{-1}_{5/2})_{4^+} \\
& ({}_{\Lambda}p_{1/2,3/2} \otimes {}_{n}d^{-1}_{5/2})_{3^-} \\
{}^{48}_{\Lambda}\mathrm{Ca}:\ & ({}_{\Lambda}f_{5/2,7/2} \otimes {}_{n}f^{-1}_{7/2})_{6^+} \\
& ({}_{\Lambda}d_{3/2,5/2} \otimes {}_{n}f^{-1}_{7/2})_{5^-}
\end{aligned} \qquad (17)$$

and so forth. In Fig. 10, we show these high spin states on a J vs. A plot, along with continuous curves corresponding to the optimum matching condition (16). The A dependence of the optimum J arises from the oscillator radius parameter b, which we have taken as proportional to $A^{1/3}$. Note that q decreases with increasing p_π (see Fig. 4), so that by varying p_π, we sweep out a band of optimum J values. The elementary $\pi^+ n \to K^+ \Lambda$ cross section[40] peaks near $p_\pi = 1.04$ GeV/c, but remains sizable up to about 1.5 GeV/c. From Fig. 10, we see that for light systems such as ${}^{28}_{\Lambda}$Si or ${}^{48}_{\Lambda}$Ca, the highest spin state is very well matched at 1.04 GeV/c, so the largest (π^+,K^+) cross sections are to be expected for these states. For heavier hypernuclei, we are no longer well matched at 1.04 GeV/c, so smaller cross sections will result. In Ref. (38), estimates of (π^+,K^+) cross sections are given for a range of targets and incident momenta, using PWA, DWIA and eikonal approximations. A typical DWIA theoretical prediction[38] is shown in Fig. 11 for ^{40}Ca (π^+,K^+) ${}^{40}_{\Lambda}$Ca* at 1.04 GeV/c. The cross sections for stretch states decrease when J is decreased, but by less than a factor of two per unit of J. Hence several states should have measurable cross sections. The results shown in Fig. 11 are reduced by only about a factor of 5-10 with respect to PWA estimates, since the K^+ is weakly absorbed in the exit channel.

The (π^+,K^+) reaction could open up a new domain of hypernuclear structure physics. The high spin "stretch" states discussed here are of a particularly simple structure, since only one Λn^{-1} configuration of the maximum J exists. In heavy systems, the "spreading width" of very high spin states will be less than that for lower spins, since there is a lower density of compound states (2p 2h, etc.) of the same spin. Thus narrow excitations may exist, even quite high in the continuum. There is as yet no experimental data on the (π^+,K^+) reactions, but an experiment is being planned[41] for the Brookhaven AGS.

As a final topic of the "futuristic" type, we consider the possibility of producing Ξ^- or $\Lambda\Lambda$ hypernuclei via the double strangeness exchange (K^-,K^+) reaction[42]. Such studies would be of fundamental interest from several points of view: a) explore a new type of hypernuclear spectroscopy; b) shed some light on the nature of ΞN and $\Lambda\Lambda$ interaction, thereby extending our knowledge of the SU(3) structure of baryon-baryon forces; c) possibility of narrow Ξ states in nuclei; and d) provide a possible test for Bag model predictions[43] of a strangeness -2 dibaryon.

Two events corresponding to double hypernucleus production are known from emulsion work[44] (${}^{6}_{\Lambda\Lambda}$He and ${}^{10}_{\Lambda\Lambda}$Be). These are identified by tracks corresponding to two successive weak decays $\Lambda\to p\pi^-$. In the case of ${}^{6}_{\Lambda\Lambda}$He, the first step is a $K^- + p \to K^+ + \Xi^-$ reaction, followed by the slowing down of the Ξ^- in the emulsion, and finally the capture process $\Xi^- + {}^{12}C \to {}^{7}Li + {}^{6}_{\Lambda\Lambda}He$.

Second order processes for the formation of $\Lambda\Lambda$ hypernuclei have been evaluated in Ref. (42). These correspond to the graphs of Fig. 12. The 0° cross section for the $K^-p\to\pi^\circ\Lambda$ followed by $\pi^\circ p\to K^+\Lambda$ reaction, summed over all final $\Lambda\Lambda$ hypernuclear states, is given[42] in rough approximation by

$$\sum_f \left(\frac{d\sigma}{d\Omega}\right)_f^{0^\circ} = \frac{8\pi^2\alpha_1\alpha_2\xi}{k_\pi^2} \left\langle\frac{1}{r^2}\right\rangle \left(\frac{d\sigma}{d\Omega_L}\right)_{0^\circ}^{K^-p\to\pi^\circ\Lambda} \left(\frac{d\sigma}{d\Omega_L}\right)_{0^\circ}^{\pi^\circ p\to K^+\Lambda} \qquad (18)$$

where

$$\alpha_1 = (1 - q^{(1)}/v_\pi E_\Lambda^{(1)})$$

$$\alpha_2 = (1 - q^{(2)}/v_{K^+} E_\Lambda^{(2)}) \tag{19}$$

$$\xi = \int \frac{d^2\vec{Q}_\perp}{(2\pi)^2} \left|\frac{t_1(\vec{Q}_\perp)}{t_1(o)}\right|^2 \left|\frac{t_2(-\vec{Q}_\perp)}{t_2(o)}\right|^2$$

Here $t_{1,2}$ are t-matrices for processes 1 and 2 and ξ takes account of their angular dependence. A Glauber approximation has been used to reduce the $d^3\vec{Q}$ integral to a two dimensional integral over $\vec{Q}_\perp$ (x,y components). The existing experimental data[44] on $\bar{K}N \to \pi\Lambda$ and $\pi N \to K\Lambda$ can be used to obtain

$$\xi \simeq 0.02 \text{ mb}^{-1}$$

$$\left(\frac{d\sigma}{d\Omega_L}\right)_{0°}^{K^- p\to\pi^\circ\Lambda} \simeq 0.76 \text{ mb/st} \tag{20}$$

$$\left(\frac{d\sigma}{d\Omega_L}\right)^{\pi^\circ p\to K^+\Lambda} \simeq 0.65 \text{ mb/st}$$

for $p_{K^-} = 1.1$ GeV/c, $p_{\pi^\circ} = 1.02$ GeV/c. This choice of momentum corresponds to the peak in the product of $d\sigma/d\Omega_L$ factors. Using the values in (20), and taking $\langle 1/r^2\rangle \simeq 3p_F^2/20 \simeq 0.028 \text{ mb}^{-1}$ from the Fermi gas model, we obtain

$$\sum_f \left(\frac{d\sigma}{d\Omega_L}\right)_f^{0°} \simeq 4\mu\text{b/st} \tag{21}$$

for the summed (K^-,K^+) cross section.

Note that the sum over states includes the quasielastic contribution, (one or both Λ's in the continuum) which is a sizable part of the total, since q is large. The contribution of discrete $\Lambda\Lambda p^{-1}p^{-1}$ states to (21) will arise mainly from high spin states. The first Λ, produced in the low q process $K^-p\to\pi^\circ\Lambda$, would have maximum "sticking probability" in a low spin state, but the second Λ, produced in the high q process $\pi^\circ p\to K^+\Lambda$, can stick only in a high spin state. Thus the (K^-,K^+) cross sections to discrete states may be too small to measure with current K-beams, although this reaction remains very promising for future facilities.

Rather than considering ΛΛ hypernucleus formation, we may look at the one step process $K^-p\to K^+\Xi$. The reaction $\Xi^-p\to\Lambda\Lambda$ then serves to provide the Ξ^- state with a conversion width, analogous to the situation for $\Sigma^-p\to\Lambda n$. The two-body threshold for the Ξ^- production is at $p_{K^-}\simeq 1.05$ GeV/c, so the formation of Ξ hypernuclei is kinematically separated from that of ΛΛ hypernuclei (the Q value for $\Xi^-p\to\Lambda\Lambda$ is 30 MeV). The summed cross section at 0° for a Ξ hypernucleus in a (K^-,K^+) reaction is[42]

$$\sum_f \left(\frac{d\sigma}{d\Omega_L}\right)^f_{0^\circ} = Z_{eff}\ \alpha\ (d\sigma/d\Omega_L)^{K^-p\to K^+\Xi^-}_{0^\circ} \tag{22}$$

where Z_{eff} is the effective proton number

$$Z_{eff} = \int \rho_p(r)\,|\chi^{(-)}_{K^-}(r)|^2\,|\chi^{(+)}_{K^+}(r)|^2 \tag{23}$$

and $\alpha = (1 - q/v_{K^+}E_{\Xi})$. In Eq. (23), $\chi^{(\pm)}$ are distorted waves obtained from the optical model. We estimate[42] Z_{eff} to be of the order of 1 and take

$$\left(\frac{d\sigma}{d\Omega_L}\right)_{0°}^{K^-p\to K^+\Xi^-} \simeq 30\ \mu b/st \qquad (24)$$

at $p_{K^-} \approx 1.26$ GeV/c, from experiment[45]. This gives

$$\left(d\sigma/d\Omega_L\right)_{0°}^{f} \simeq \mu b/st \qquad (25)$$

for Ξ hypernucleus formation. Since q $\simeq$ 400 MeV/c, only discrete Ξ states of high spin will be populated in the (K^-,K^+) reaction. The quasielastic process represents much of the sum of Eq. (25).

The Hartree potential for a Ξ in the nucleus and the width Γ_Ξ arising from $\Xi^- p\to\Lambda\Lambda$ have been estimated in Ref. (42). Because of the smaller phase space for the conversion process, Ξ widths are intrinsically smaller than Σ widths. The quenching mechanism discussed earlier for Σ widths[25] also operates for the Ξ, since at low energies, the process $\Xi^- p\to\Lambda\Lambda$ takes place only from the I = 0, $^1S_0$ channel. Very narrow Ξ states may thus be anticipated[42]. Intense kaon beams are required to find them!

There are also a number of unique possibilites for the K^+ as a probe of nuclear structure. The K^+ does not transfer strangeness to the nucleus, but its weak absorption makes it distinctive among hadrons. Its features have been discussed in some detail in the literature,[5,46-48] so we only give a skeleton outline here. The K^+ should in principle be useful for a) extraction of information on neutron densities[5,47] from elastic scattering, as well as spin flip form factors[47]. This requires a good knowledge of the elementary K^+N amplitudes; b) K^+ inelastic scattering studies of giant isoscalar 0^+ and 2^+ resonances and high spin unnatural parity states. It would be interesting to compare these results to π, p and e^-

inelastic scattering to the same class of states; c) charge exchange (K^+,K^o) reactions[5] to look at the isospin structure of giant resonances; d) investigation of nucleon quasiparticle properties via the (K^+,K^+p) knockout reaction[49], and comparison with (e,e'p) and (p,2p) results. There is some recent data[50] on $K^\pm$ elastic scattering on ^{12}C and ^{40}Ca at 800 MeV/c. These data have been discussed in the context of the optical model[48]. A first order potential (linear in the nuclear density $\rho(r)$) with no free parameters gave excellent agreement[48] with the K^+ elastic scattering data.

I have tried to indicate some of the interesting questions which arise in kaon-nucleus physics, but the list has been far from complete. There are many open questions and opportunities for advances in our understanding of how strange mesons and baryons interact with nuclei.

References:

1. A. Gal, in Advances in Nuclear Physics, Vol. 8, Eds. M. Baranger and E. Vogt, Plenum Press, New York (1975), pp. 1-120.

2. C. B. Dover, Proceedings of the Kaon Factory Workshop, Vancouver, B. C., Canada, August, 1979, Ed. M. K. Craddock, TRIUMF Report TRI-79-1, pp. 4-11.

3. B. Povh, Reports on Progress in Physics 39, 824 (1976); Ann. Rev. Nucl. Part. Sci. 28, 1 (1978).

4. B. Povh, "Nuclear Physics with Hyperons", Max Planck Institute Preprint MPI H-1979-V25.

5. C. B. Dover and P. J. Moffa, Phys. Rev. C16, 1087 (1977); C. B. Dover and G. E. Walker, Phys. Rev. C19, 1393 (1979).

6. K. K. Li, Proceedings of the Topical Conference on Meson-Nuclear Physics, Carnegie Mellon University, May 1976; T. Kycia and K. K. Li, private communication.

7. K. K. Li, private communication; the data points are from a Brookhaven experiment; the solid lines are based on the analysis of B. R. Martin, Nucl. Phys. B94, 413 (1975).

8. C. B. Dover, Proceedings of the International Topical Conference on Meson-Nuclear Physics, Houston, March, 1979; AIP Conf. Proc. No. 54, Ed. E. V. Hungerford III, p. 634-657.

9. H. Feshbach and A. K. Kerman, Preludes in Theoretical Physics (Amsterdam, North Holland, 1965), p. 260.

10. G. C. Bonazzola et al, Phys. Rev. Lett. 34, 683 (1975); W. Brückner et al, Phys. Lett. 62B, 481 (1976).

References:

11. W. Brückner et al, Phys. Lett. 79B, 157 (1978).

12. R. Chrien et al, Phys. Lett. 89B, 31 (1979).

13. C. B. Dover, A. Gal, G. E. Walker and R. H. Dalitz, Phys. Lett. 89B, 26 (1979).

14. J. Hüfner, S. Y. Lee and H. A. Weidenmüller, Nucl. Phys. A234, 429 (1974).

15. A. Bouyssy, Nucl. Phys. A290, 324 (1977).

16. J. Pniewski and D. Zieminska, Proceedings of the Seminar on Kaon-Nuclear Interaction and Hypernuclei, Zvenigorod, Russia, September 1977, pp. 33-50.

17. A. Bouyssy, Phys. Lett. 84B, 41 (1979).

18. R. Brockmann and W. Weise, Phys. Lett. 69B, 167 (1977).

19. H. J. Pirner, Phys. Lett. 85B, 190 (1979).

20. J. V. Noble, Phys. Lett. 89B, 327 (1980).

21. A. Gal, J. M. Soper and R. H. Dalitz, Ann. Phys. 66, 63 (1971); 72, 445 (1972).

22. R. Bertini, Proceedings of the Second International Conference on Meson-Nuclear Physics, Houston, March 1979, AIP Conf. Proc. No. 54, Ed. E. V. Hungerford III, pp. 703-713.

23. M. Nagels, Nijmegan Thesis (1975); M. Nagels, T. A. Rijken and J. J. deSwart, Phys. Rev. D15, 2547 (1977).

24. These Σ widths were actually obtained by solving for the complex eigenvalues of the Schrödinger equation, using a first order ($t\rho$) approximation to the Σ optical potential.

References:

25. A. Gal and C. B. Dover, Phys. Rev. Lett. 44, 379 (1980).

26. M. Bedjidian et al, Phys. Lett. 83B, 252 (1979).

27. M. Bedjidian et al, Phys. Lett., to be published.

28. R. H. Dalitz and A. Gal, Ann. Phys. 116, 167 (1978).

29. A. Bamberger et al, Nucl. Phys. B60, 1 (1973).

30. P. Birien, in Proceedings of the International Conference on Hypernuclear and Low Energy Kaon Physics, Jablonna, Poland, September 1979; to appear in Nukleonika (1980).

31. Proceedings of the Kaon Factory Workshop, Vancouver, B. C., Canada, August 1979, Ed. M. K. Craddock, TRIUMF Report TRI-79-1.

32. Proceedings of the Summer Study Meeting on Nuclear and Hypernuclear Physics with Kaon Beams, Brookhaven National Laboratory, July 1973; Ed. H. Palevsky, BNL 18335.

33. Proceedings of the Summer Study Meeting on Kaon Physics and Facilities, Brookhaven National Laboratory, June, 1976; Ed. H. Palevsky, BNL 50579.

34. See Ref. 2.

35. A. K. Kerman and H. J. Lipkin, Ann. Phys. 66, 738 (1971).

36. L. S. Kisslinger and N. V. Giai, Phys. Lett. 72B, 19 (1977).

37. R. H. Dalitz and A. Gal, Phys. Rev. Lett. 36, 362 (1976).

38. C. B. Dover, L. Ludeking and G. E. Walker, preprint (1980).

39. M. Rayet, Ann. Phys. 102, 226 (1976).

40. R. D. Baker et al, Nucl. Phys. B126, 365 (1977); Nucl. Phys. B141, 29, (1978); D. H. Saxon et al, Rutherford Lab preprint, July 1979.

References:

41. A. Thiessen, private communication.

42. C. B. Dover, Proceedings of the International Conference on Hypernuclear and Low Energy Kaon Physics, Jablonna, Poland, September 1979; C. B. Dover and A. Gal, in preparation.

43. R. Jaffe, Phys. Rev. Lett. 38, 195 (1977).

44. A. J. Van Horn et al, Phys. Rev. D6, 1275 (1972); J. Keren, Phys. Rev. 133, B457 (1964).

45. G. Burgun et al, Nucl. Phys. B8, 447 (1968).

46. C. B. Dover and G. E. Walker, Phys. Reports C, in preparation.

47. S. R. Cotanch, Nucl. Phys. A308, 253 (1978); Phys. Rev. C18, 1941 (1978).

48. A. S. Rosenthal and F. Tabakin, Phys. Rev. C (to be published).

49. R. D. Koshel, P. J. Moffa and E. F. Redish, Phys. Rev. Lett. 39, 1319 (1977).

50. R. Eisenstein, Ref. (2), pp. 75-81.

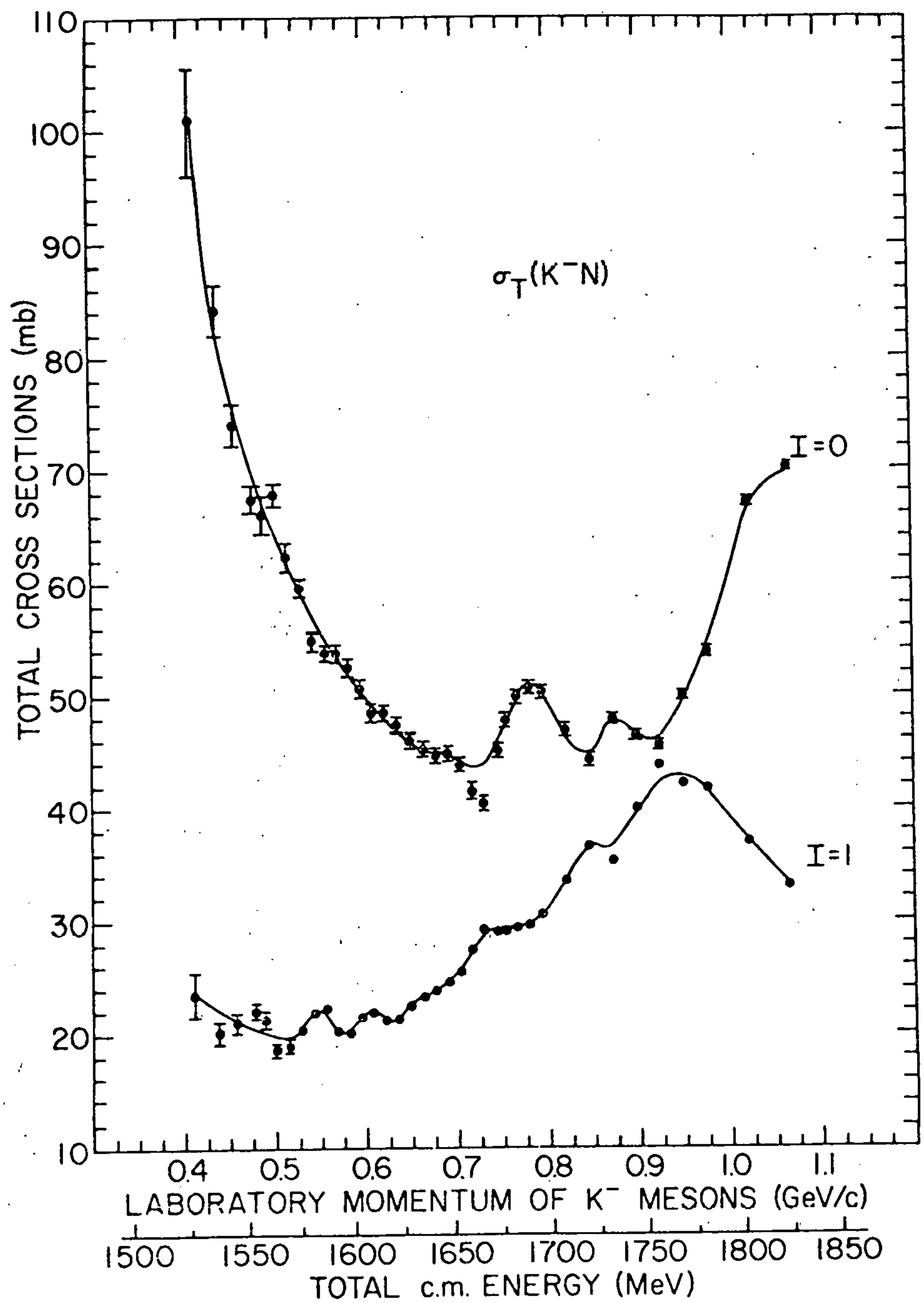

110
100
90
80
70
60
50
40
30
20
10
TOTAL CROSS SECTIONS (mb)
σT(K⁻N)
I=0
I=1
0.4
0.5
0.6
0.7
0.8
0.9
1.0
1.1
LABORATORY MOMENTUM OF K⁻ MESONS (GeV/c)
1500
1550
1600
1650
1700
1750
1800
1850
TOTAL c.m. ENERGY (MeV)

Figure 1

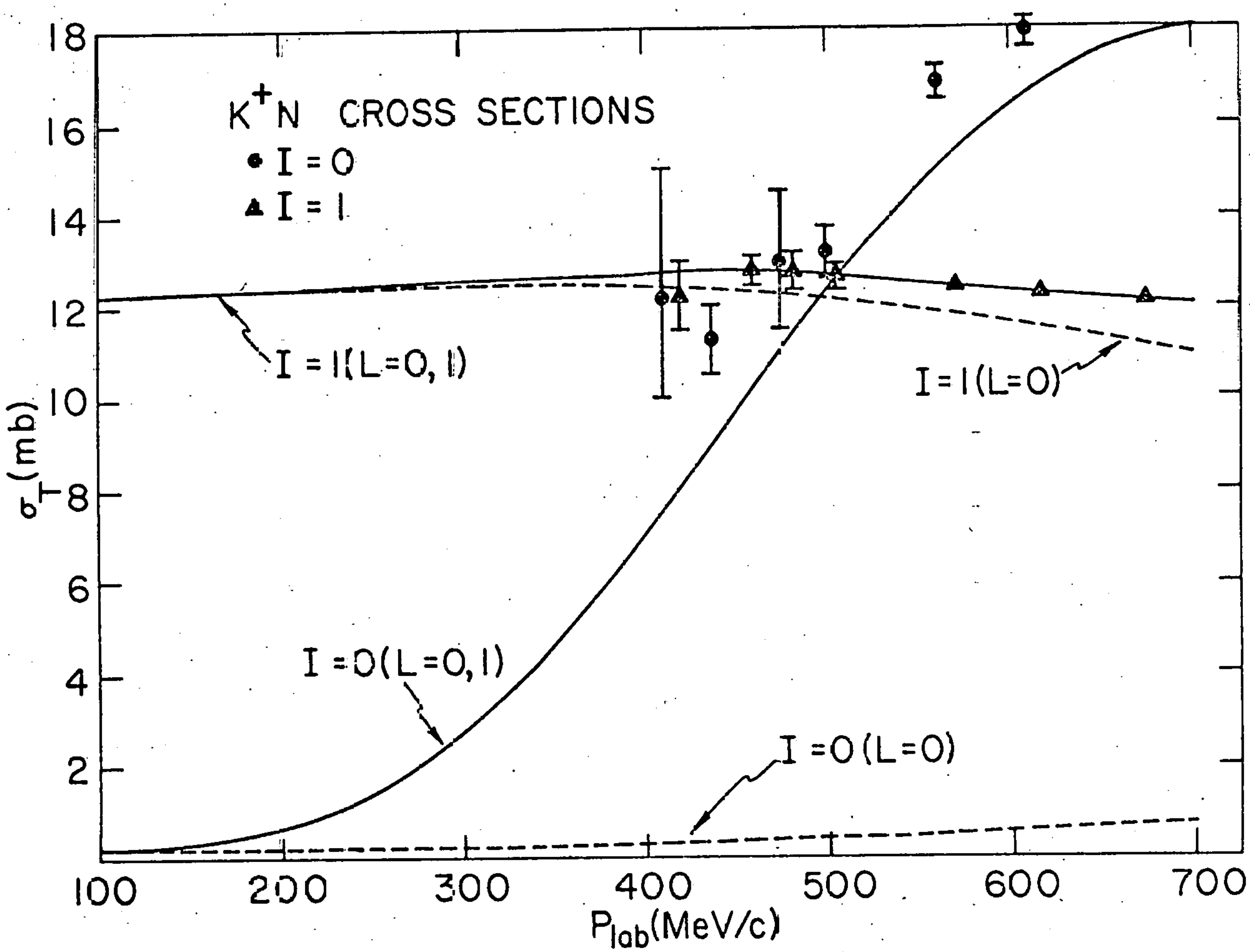
K+N CROSS SECTIONS
I = 0
I = 1
I = 1(L=0,1)
I = 1(L=0)
I = 0(L=0,1)
I = 0(L=0)
σT(mb)
Plab(MeV/c)
18
16
14
12
10
8
6
4
2
100
200
300
400
500
600
700

Figure 2

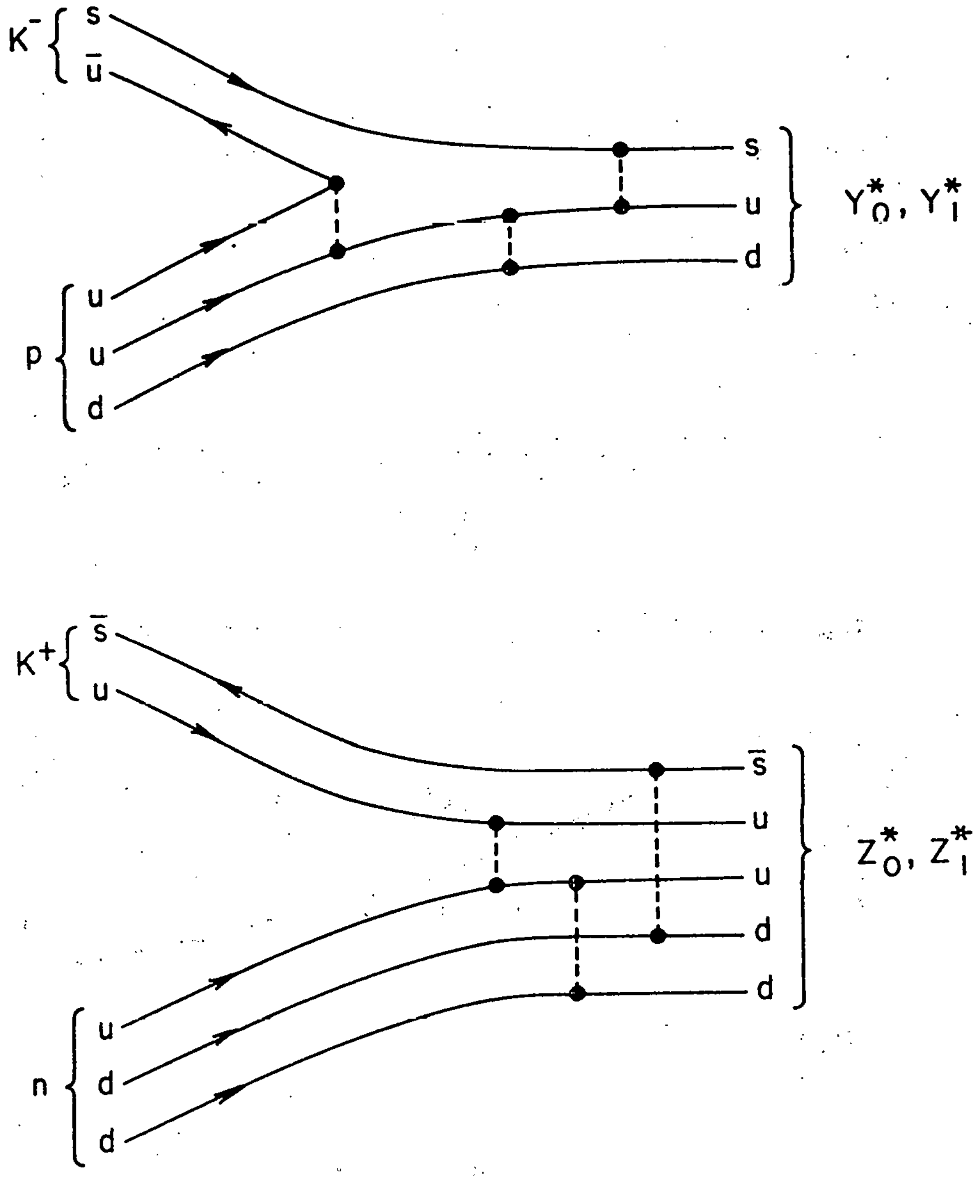

Figure 3

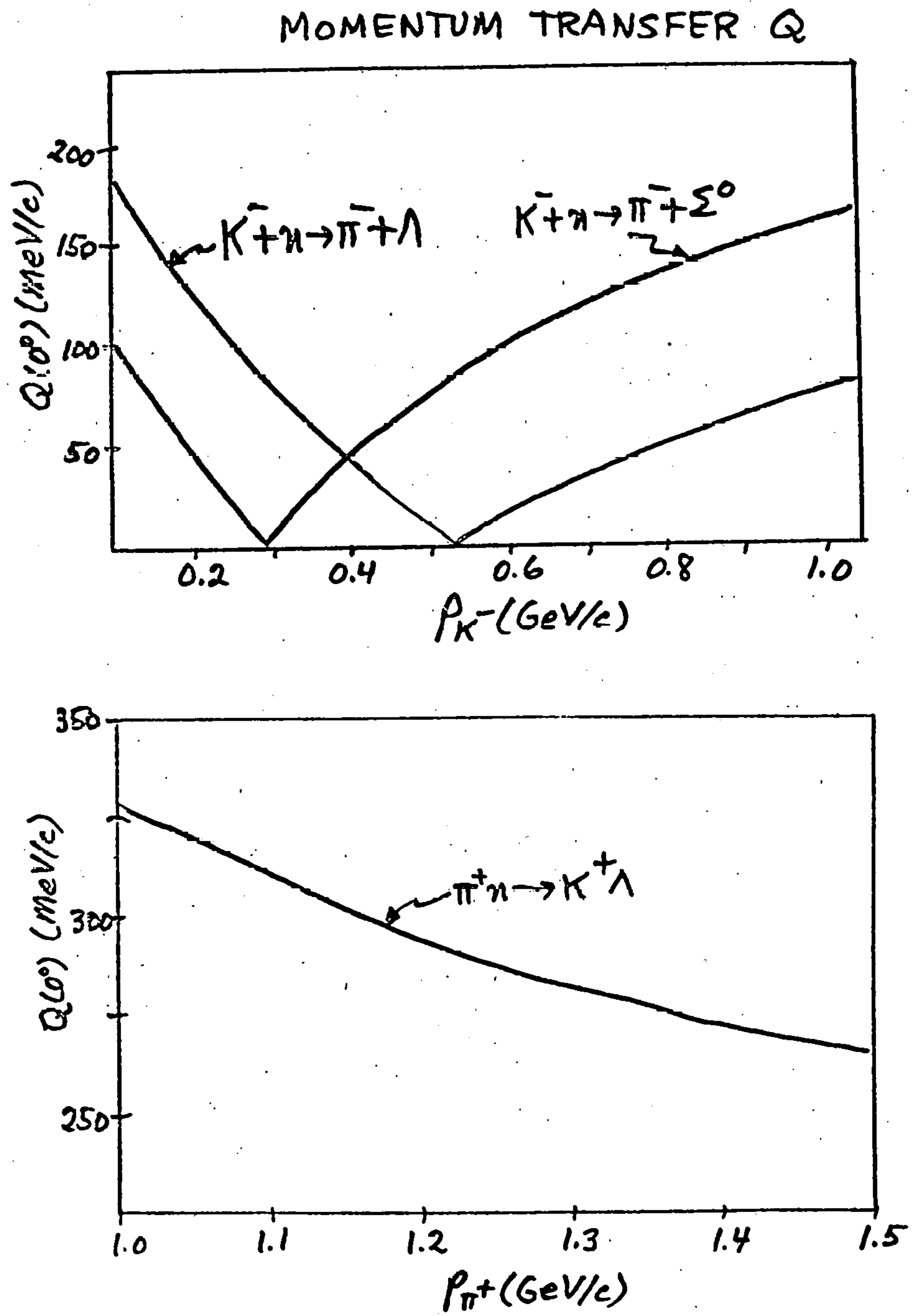

MOMENTUM TRANSFER Q
K⁻+n→π⁻+Λ
K⁻+n→π⁻+Σ⁰
Q(0°) (MeV/c)
200
150
100
50
0.2
0.4
0.6
0.8
1.0
p_K⁻ (GeV/c)
π⁺n→K⁺Λ
Q(0°) (MeV/c)
350
300
250
1.0
1.1
1.2
1.3
1.4
1.5
p_π⁺ (GeV/c)

Figure 4

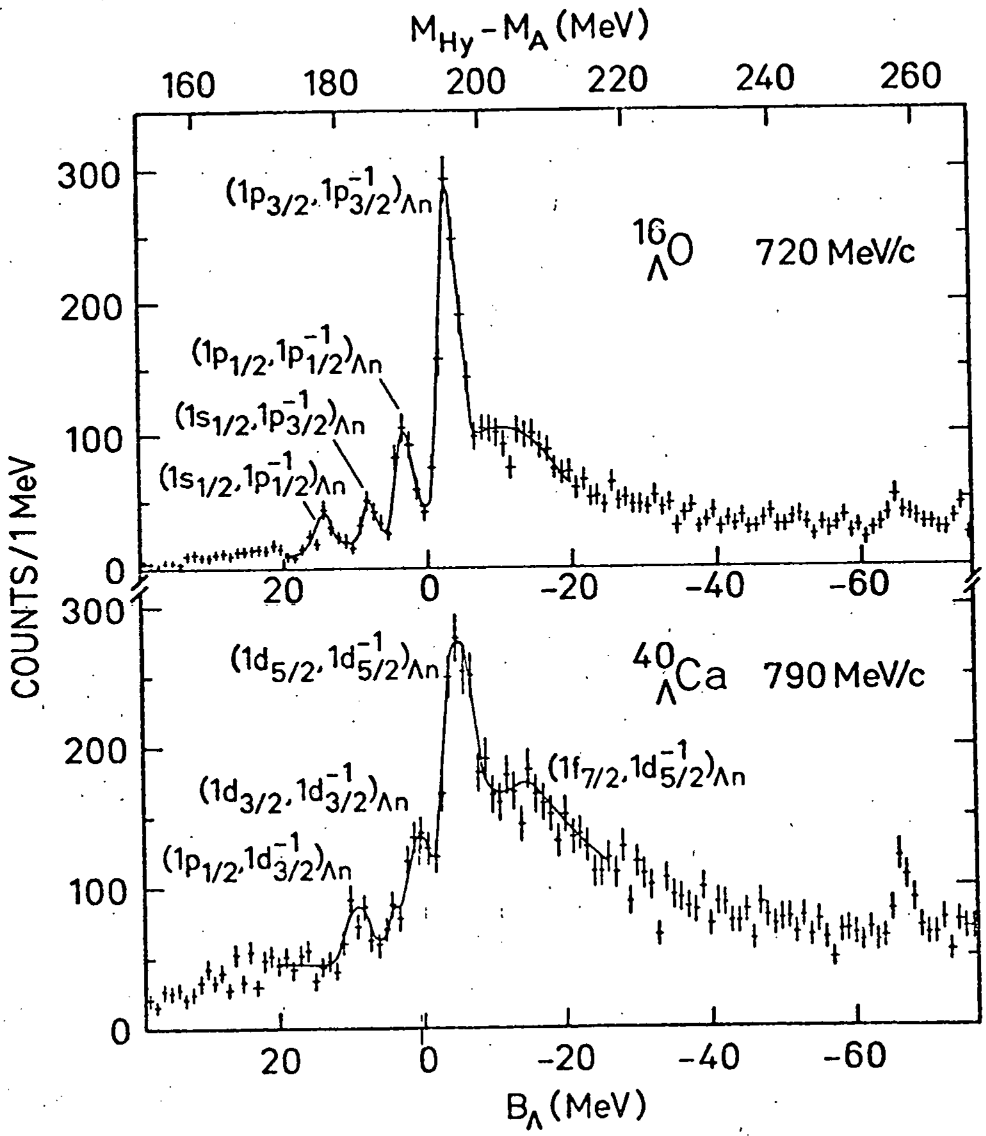

M_Hy - M_A (MeV)
160
180
200
220
240
260
300
200
100
0
COUNTS/1 MeV
(1p3/2, 1p-1 3/2)Λn
16 Λ O
720 MeV/c
(1p1/2, 1p-1 1/2)Λn
(1s1/2, 1p-1 3/2)Λn
(1s1/2, 1p-1 1/2)Λn
20
0
-20
-40
-60
300
(1d5/2, 1d-1 5/2)Λn
40 Λ Ca
790 MeV/c
200
(1d3/2, 1d-1 3/2)Λn
(1f7/2, 1d-1 5/2)Λn
(1p1/2, 1d-1 3/2)Λn
100
0
20
0
-20
-40
-60
BΛ (MeV)

Figure 5

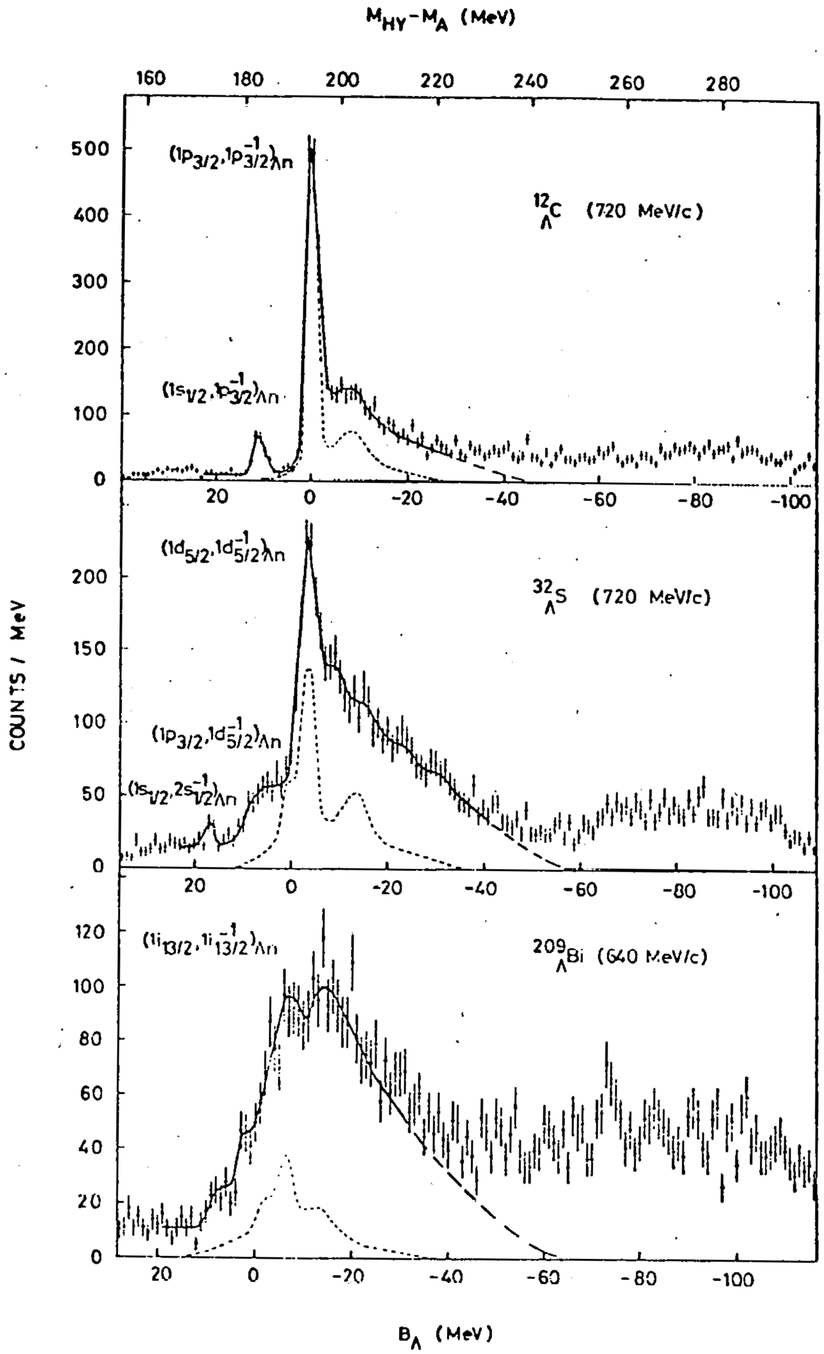

$M_{HY}-M_A$ (MeV)
COUNTS / MeV
$(1p_{3/2},1p_{3/2}^{-1})_{\Lambda n}$
$^{12}_{\Lambda}C$ (720 MeV/c)
$(1s_{1/2},1p_{3/2}^{-1})_{\Lambda n}$
$(1d_{5/2},1d_{5/2}^{-1})_{\Lambda n}$
$^{32}_{\Lambda}S$ (720 MeV/c)
$(1p_{3/2},1d_{5/2}^{-1})_{\Lambda n}$
$(1s_{1/2},2s_{1/2}^{-1})_{\Lambda n}$
$(1i_{13/2},1i_{13/2}^{-1})_{\Lambda n}$
$^{209}_{\Lambda}Bi$ (640 MeV/c)
B_{Λ} (MeV)

Figure 6

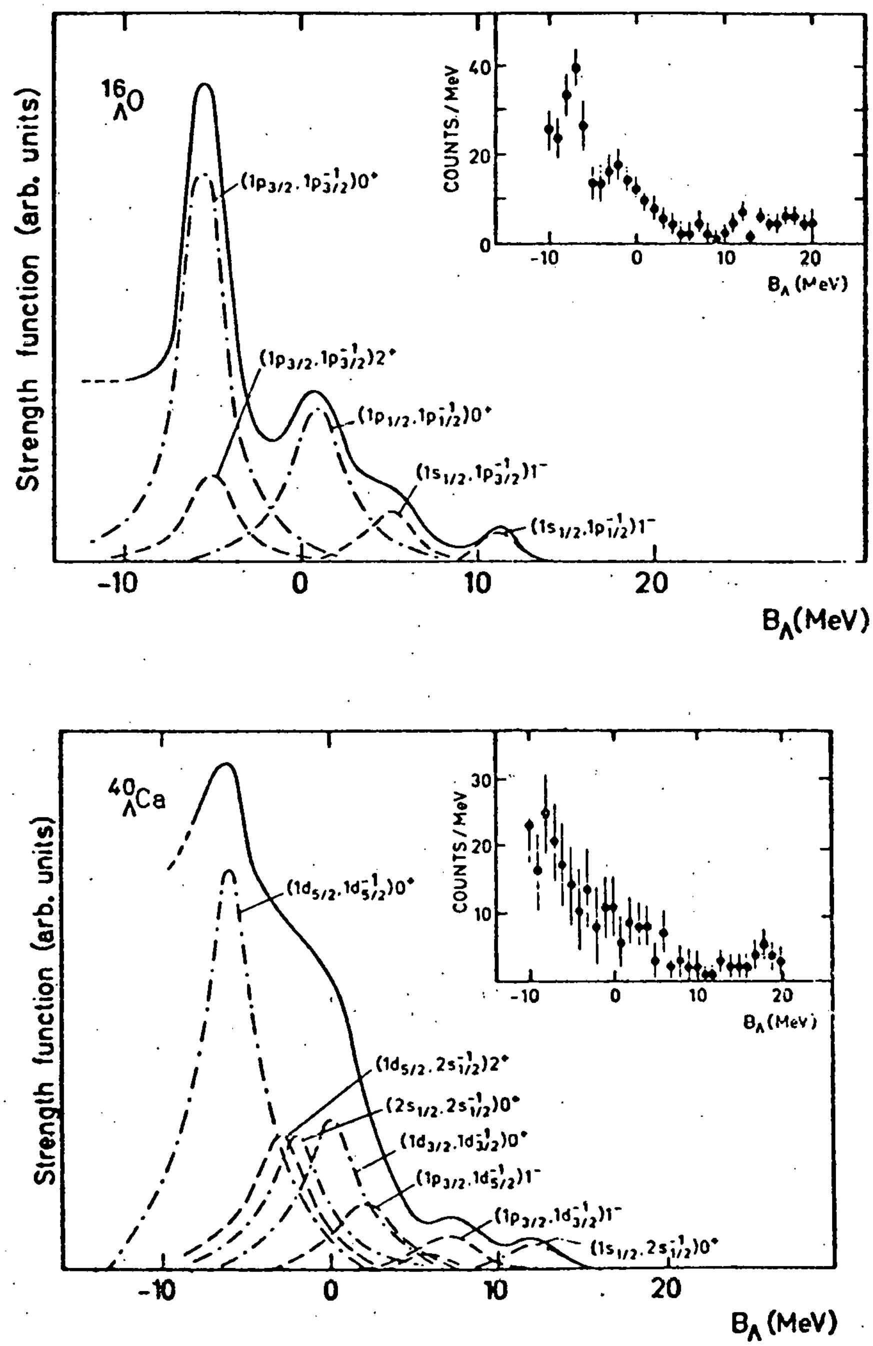

${}^{16}_{\Lambda}O$
Strength function (arb. units)
$(1p_{3/2}.1p_{3/2}^{-1})0^+$
$(1p_{3/2}.1p_{3/2}^{-1})2^+$
$(1p_{1/2}.1p_{1/2}^{-1})0^+$
$(1s_{1/2}.1p_{3/2}^{-1})1^-$
$(1s_{1/2}.1p_{1/2}^{-1})1^-$
-10
0
10
20
B_Λ(MeV)
COUNTS/MeV
40
20
0
-10
0
10
20
B_Λ (MeV)
${}^{40}_{\Lambda}Ca$
Strength function (arb. units)
$(1d_{5/2}.1d_{5/2}^{-1})0^+$
$(1d_{5/2}.2s_{1/2}^{-1})2^+$
$(2s_{1/2}.2s_{1/2}^{-1})0^+$
$(1d_{3/2}.1d_{3/2}^{-1})0^+$
$(1p_{3/2}.1d_{5/2}^{-1})1^-$
$(1p_{3/2}.1d_{3/2}^{-1})1^-$
$(1s_{1/2}.2s_{1/2}^{-1})0^+$
-10
0
10
20
B_Λ (MeV)
COUNTS/MeV
30
20
10
-10
0
10
20
B_Λ (MeV)

Figure 7

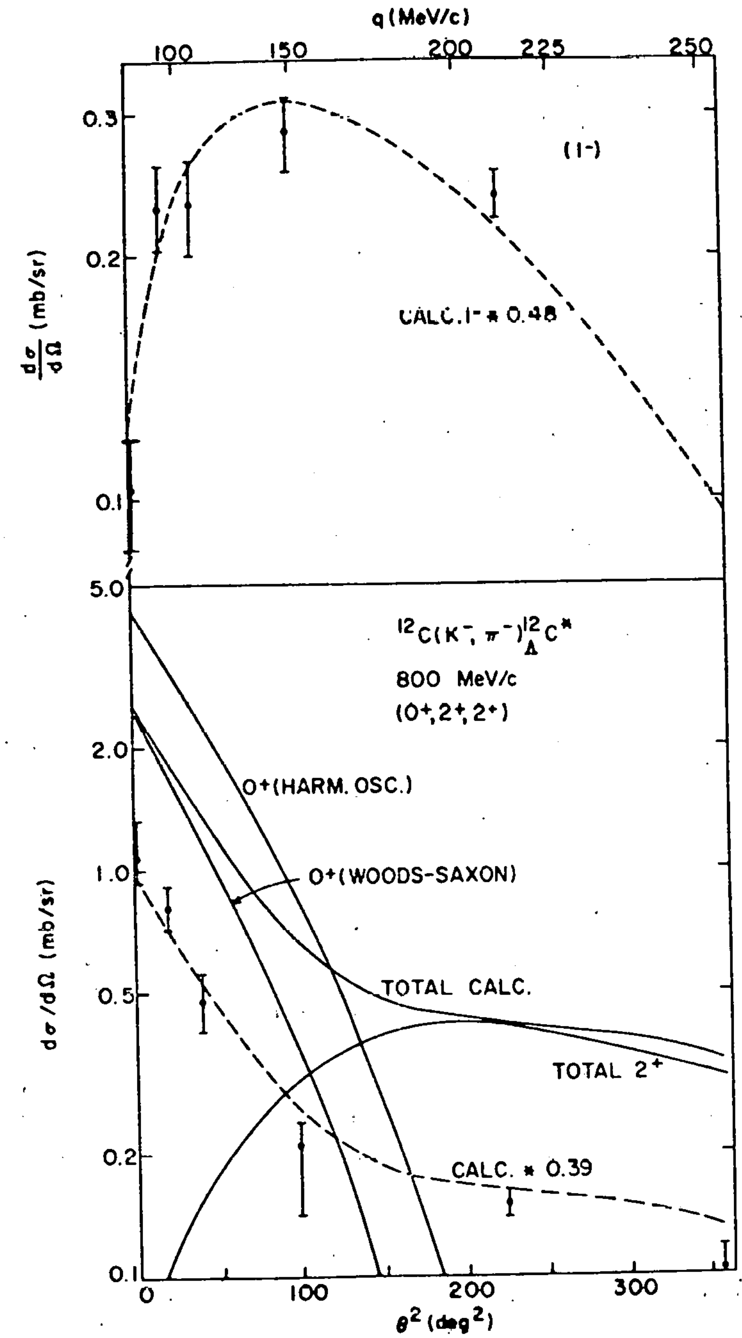
q (MeV/c)
100
150
200
225
250
0.3
0.2
0.1
(1-)
CALC. 1- * 0.48
dσ/dΩ (mb/sr)
5.0
$^{12}C(K^-, \pi^-)^{12}_{\Lambda}C^*$
800 MeV/c
(0+, 2+, 2+)
2.0
1.0
0.5
0.2
0.1
0+ (HARM. OSC.)
0+ (WOODS-SAXON)
TOTAL CALC.
TOTAL 2+
CALC. * 0.39
dσ/dΩ (mb/sr)
0
100
200
300
θ² (deg²)

Figure 8

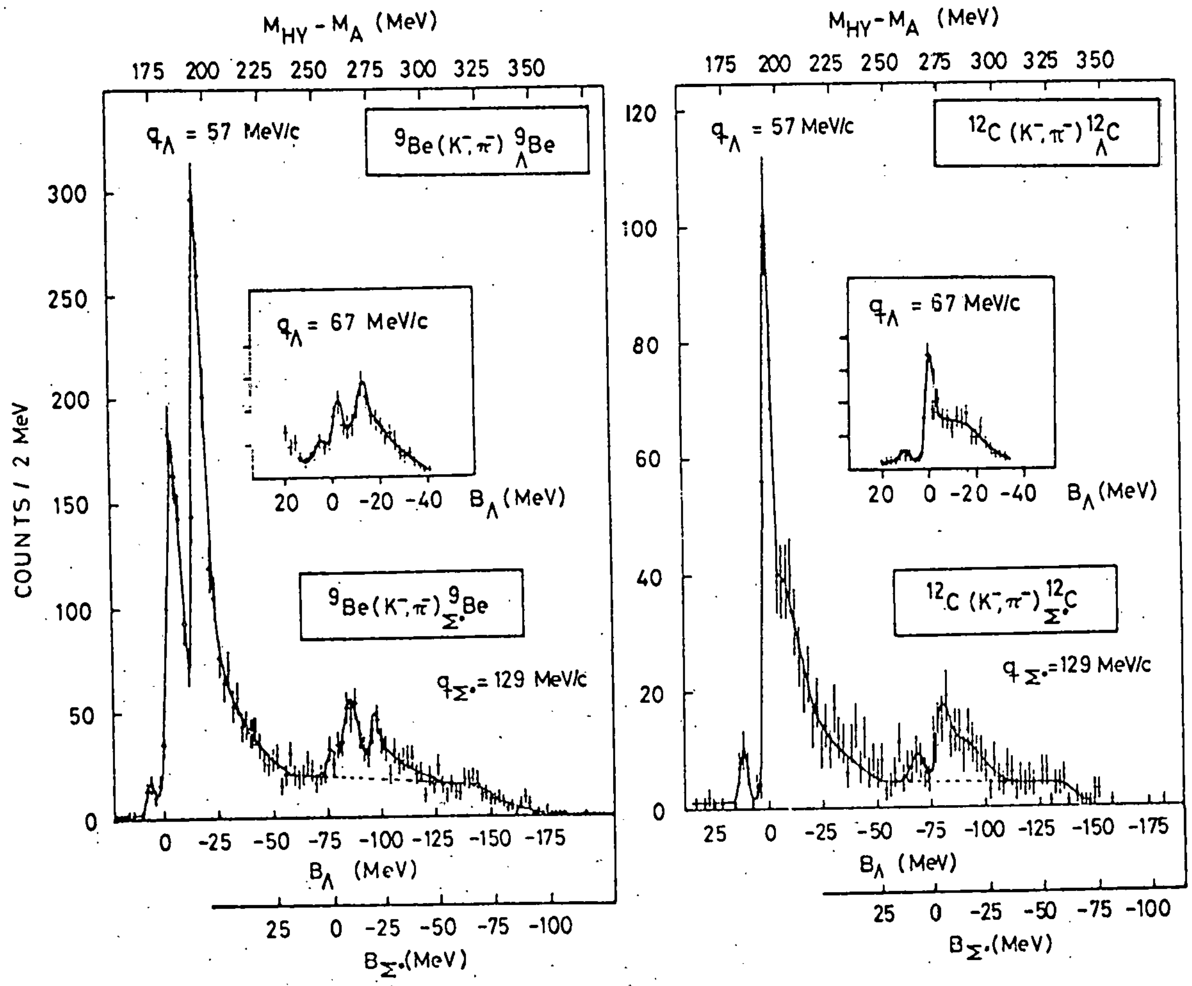
M_HY - M_A (MeV)
175 200 225 250 275 300 325 350
q_Λ = 57 MeV/c
9Be(K⁻,π⁻) 9ΛBe
q_Λ = 67 MeV/c
20 0 -20 -40 B_Λ (MeV)
9Be(K⁻,π⁻) 9Σ°Be
q_Σ° = 129 MeV/c
COUNTS / 2 MeV
300
250
200
150
100
50
0
0 -25 -50 -75 -100 -125 -150 -175
B_Λ (MeV)
25 0 -25 -50 -75 -100
B_Σ° (MeV)
M_HY - M_A (MeV)
175 200 225 250 275 300 325 350
120
100
80
60
40
20
0
q_Λ = 57 MeV/c
12C (K⁻,π⁻) 12ΛC
q_Λ = 67 MeV/c
20 0 -20 -40 B_Λ (MeV)
12C (K⁻,π⁻) 12Σ°C
q_Σ° = 129 MeV/c
25 0 -25 -50 -75 -100 -125 -150 -175
B_Λ (MeV)
25 0 -25 -50 -75 -100
B_Σ° (MeV)

Figure 9

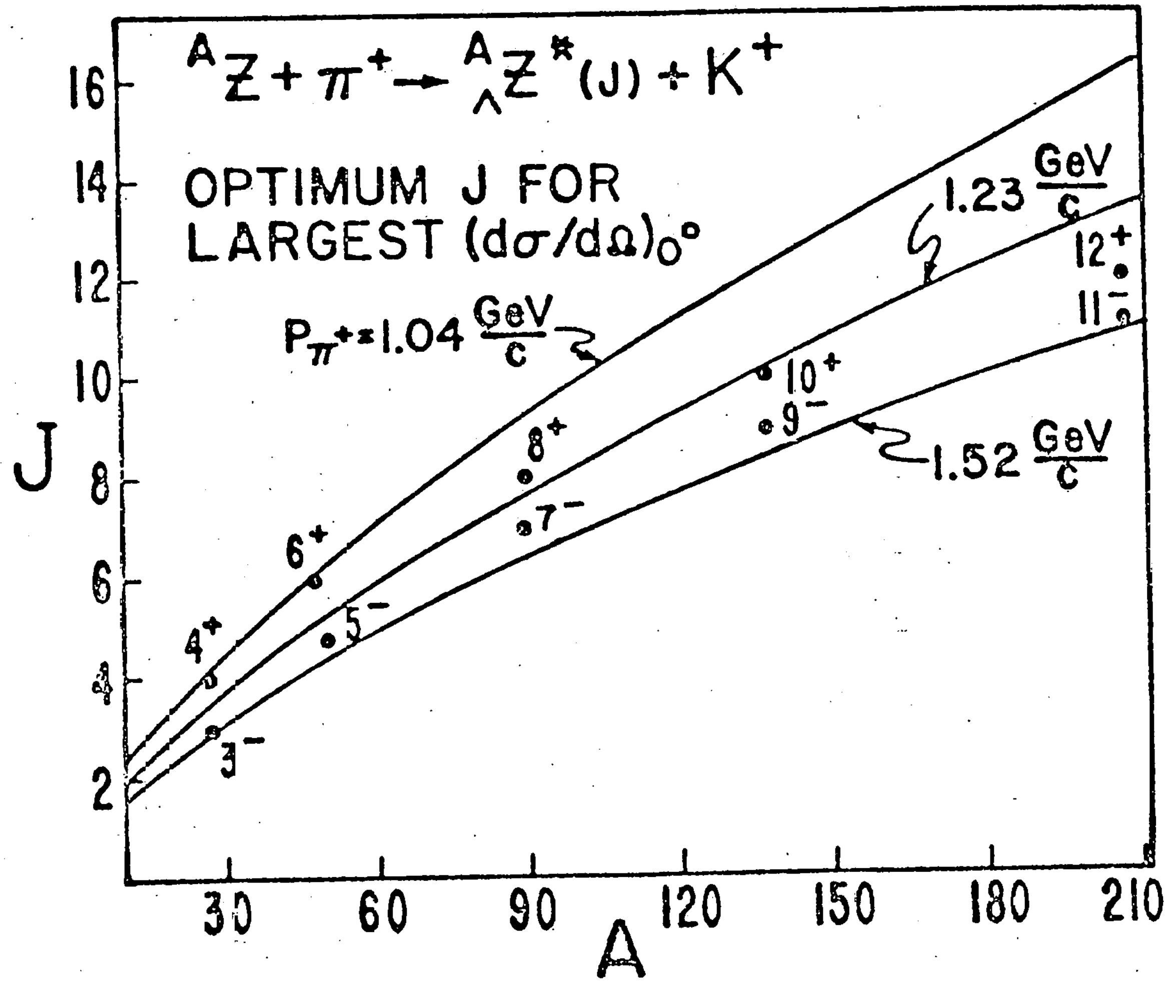

$^{A}Z + \pi^{+} \rightarrow {}^{A}_{\Lambda}Z^{*}(J) + K^{+}$
OPTIMUM J FOR
LARGEST $(d\sigma/d\Omega)_{0°}$
$P_{\pi^{+}} = 1.04 \frac{GeV}{c}$
$1.23 \frac{GeV}{c}$
$1.52 \frac{GeV}{c}$
4^{+}
3^{-}
6^{+}
5^{-}
8^{+}
7^{-}
10^{+}
9^{-}
12^{+}
11^{-}
J
A
2
4
6
8
10
12
14
16
30
60
90
120
150
180
210

Figure 10

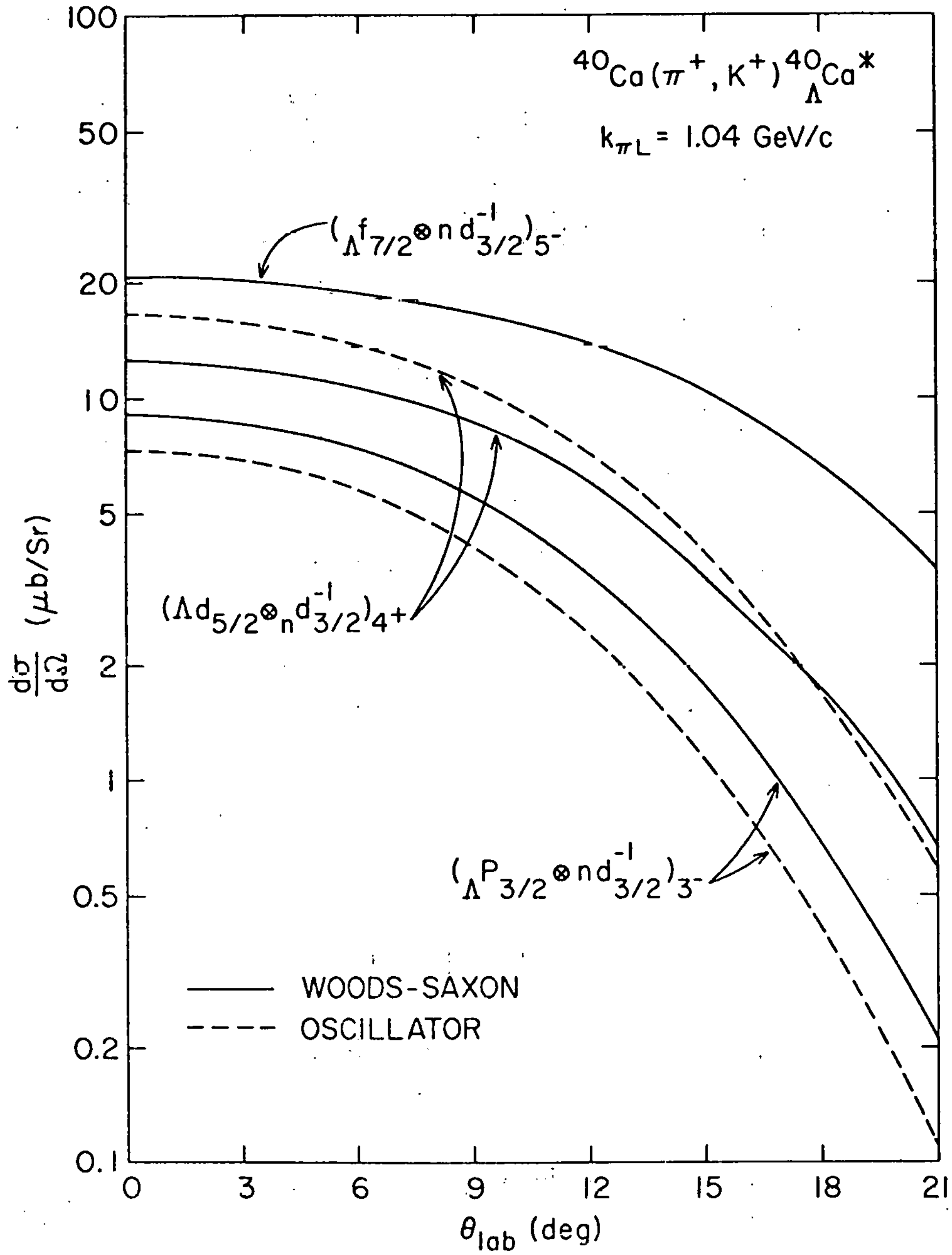
$^{40}Ca(\pi^+, K^+)^{40}_{\Lambda}Ca^*$
$k_{\pi L}$ = 1.04 GeV/c
$(_{\Lambda}f_{7/2} \otimes nd^{-1}_{3/2})_{5^-}$
$(\Lambda d_{5/2} \otimes nd^{-1}_{3/2})_{4^+}$
$(_{\Lambda}P_{3/2} \otimes nd^{-1}_{3/2})_{3^-}$
WOODS-SAXON
OSCILLATOR
$\frac{d\sigma}{d\Omega}$ (μb/Sr)
θ_{lab} (deg)
100
50
20
10
5
2
1
0.5
0.2
0.1
0
3
6
9
12
15
18
21

Figure 11

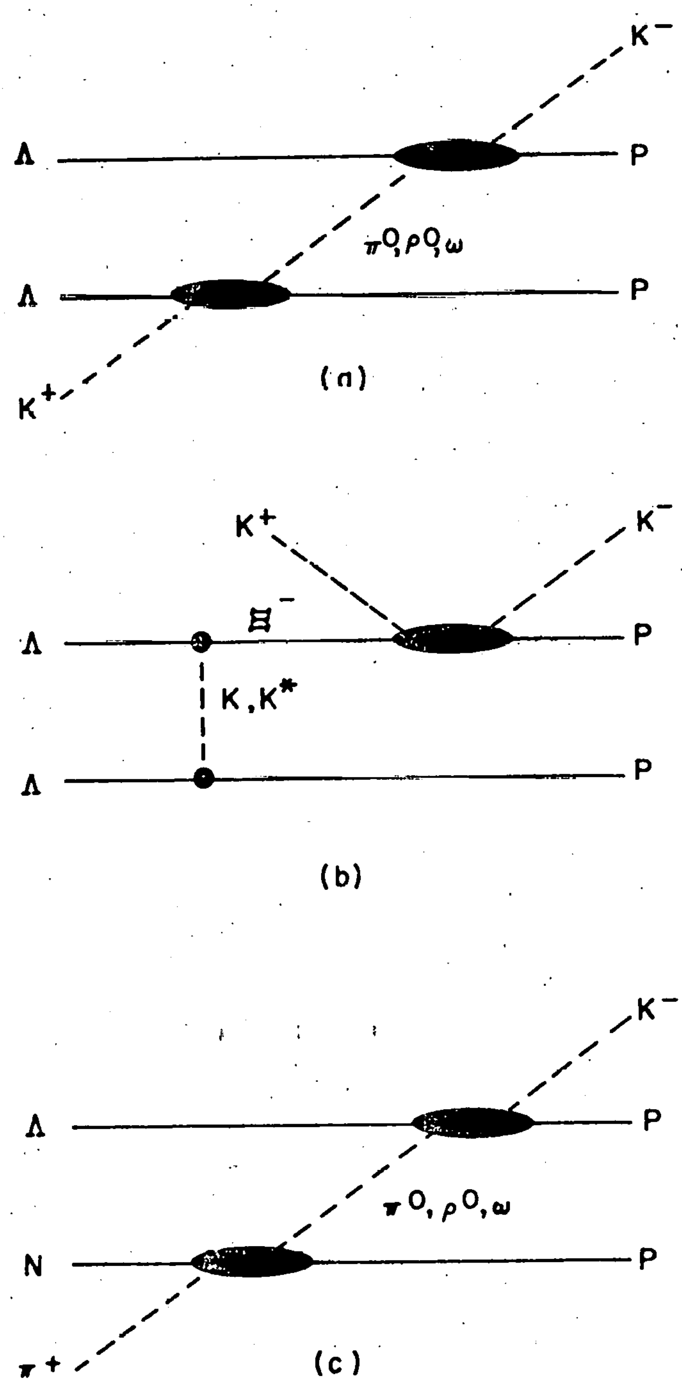

Figure 12